Journal of Alloys and Compounds 505 (2010) 302–308

Contents lists available at ScienceDirect

Journal of Alloys and Compounds

journal homepage: www.elsevier.com/locate/jallcom

Thermodynamic stabilities of strontium and barium cerates using Knudsen effusion quadrupole mass spectrometry

S.K. Rakshit, S.C. Parida*, Mohini, Ziley Singh, B.K. Sen

Product Development Division, Bhabha Atomic Research Centre, Mumbai 400085, India

ARTICLE INFO

Article history:
Received 15 February 2010
Received in revised form 1 June 2010
Accepted 8 June 2010
Available online 17 June 2010

Keywords:
Strontium cerate
Barium cerate
Proton conducting oxides
Solid oxide fuel cell
Knudsen effusion method
Quadrupole mass spectrometry
Thermodynamic properties

ABSTRACT

A Knudsen effusion cell coupled to a quadrupole mass spectrometer was calibrated by measuring the ion intensities of CO_2^+ peak over the phase mixture $\{BaCO_3(s) + BaO(s)\}$ at different temperatures. The instrument constant (K_{inst}) was calculated by comparing the ion intensities with the partial pressure data for this phase mixture taken from the literature. Subsequently, the ion intensities of CO_2^+ peak over the phase mixture $\{SrCO_3(s) + SrO(s)\}$ was measured and the partial pressure of $CO_2(g)$ over this phase mixture was calculated using this instrument constant. The enthalpy of reaction ($\Delta_r H_m^\circ$) was calculated and compared with the literature data which was found to be in excellent agreement. After validating this method by the above measurements, the partial pressure of $CO_2(g)$ over the equilibrium phase mixtures of $\{BaCeO_3(s) + BaCO_3(s) + CeO_2(s)\}$, $\{SrCeO_3(s) + SrCO_3(s) + CeO_2(s)\}$, $\{Sr_2CeO_4(s) + 2SrCO_3(s) + CeO_2(s)\}$ and $\{Sr_2CeO_4(s) + SrCO_3(s) + SrCeO_3(s)\}$were determined as a function of temperature. These partial pressure data were used in conjunction with auxiliary thermodynamic data from the literature to determine the standard molar Gibbs energies of formations of three ternary oxides $BaCeO_3(s)$, $SrCeO_3(s)$ and $Sr_2CeO_4(s)$. The thermodynamic data shows that at a particular pressure of $CO_2(g)$, $BaCeO_3(s)$ is more prone to form $BaCO_3(s)$ as compared to $SrCeO_3(s)$ to form $SrCO_3(s)$. This is an importnat asseseement since these cerates doped with rare-earths are potential proton conducting ceramic oxides used as electrolytes in solid oxide fuel cells.

1. Introduction

Ceria based ternary oxides of barium and strontium such as $BaCeO_3(s)$ and $SrCeO_3(s)$ have gained much importance due to their wide applications in solid oxide fuel cell (SOFC), hydrogen sensors, hydrogen extractors from gas mixtures, oxygen sensors and inorganic pigments [1–5]. A SOFC system usually utilizes a solid ceramic as the electrolyte and operates at higher temperature around 800 °C. SOFCs consist of two electrodes sandwiched around a hard ceramic electrolyte such as yttria stabilized zirconia [6–9]. In SOFC, hydrogen is fed into the anode of fuel cell and oxygen from the air enters into the cell through the cathode and the overall cell reaction leads to the formation of H_2O. Depending on the type of electrolyte, SOFC can be classified into two types: (1) oxide ion conducting SOFC; (2) proton conducting SOFC. The generation of water on fuel side dilutes the fuel in oxide ion conducting electrolyte and thus decreases the efficiency of the cell. These also require very high operating temperatures (>800 °C), consume large energy which is undesirable. To overcome these problems, the concept of proton conducting ceramic oxides has gained much importance as an electrolytic medium. Out of various options, rare-earth doped $SrCeO_3(s)$ and $BaCeO_3(s)$ are found to have high proton conductivities in moist environment. The proton conduction in these ceramic oxides arises due to defect reactions. Proton defects in the oxide are created when the oxide containing oxygen ion vacancies dissociate and absorb water from a surrounding wet atmosphere. In proton conducting SOFCs, water is formed on cathode, i.e. on air side, therefore, dilution of fuel does not occur and operating temperature of these cell is also low compared to oxide ion conducting SOFCs. These proton conducting ceramics such as $BaCeO_3(s)$ and $SrCeO_3(s)$ are very prone to form carbonates even with low concentration of $CO_2(g)$ which in turn decreases their stability. Sr_2CeO_4 has luminescence properties when excited with UV light, cathode rays and X-rays [10]. It has also been established that un-doped and doped $Sr_2CeO_4(s)$ act as efficient blue-white and red phosphor materials [11].

A large number of literature reports are available related to the synthesis and thermodynamic stability of these cerates with respect to their constituent binary oxides [12–15]. But, the stability of these cerates has not been determined with respect to their carbonate formation. In this study, an attempt has been made to study the stability of $BaCeO_3(s)$, $SrCeO_3(s)$ and $Sr_2CeO_4(s)$ with respect

* Corresponding author. Tel.: +91 22 2559 0648; fax: +91 22 2550 5151.
E-mail address: sureshp@barc.gov.in (S.C. Parida).

0925-8388/$ – see front matter © 2010 Elsevier B.V. All rights reserved.
doi:10.1016/j.jallcom.2010.06.057

to their carbonate formation using Knudsen Effusion Quadrupole Mass Spectrometry (KEQMS).

2. Experimental

2.1. Materials preparation

$BaCeO_3(s)$, $SrCeO_3(s)$ and $Sr_2CeO_4(s)$ were prepared using conventional solid state reaction method. Stoichiometric proportions of $BaCO_3(s)$, $SrCO_3(s)$ (LEICO Industries Inc., USA, mass fraction 0.9999) and $CeO_2(s)$ (Indian Rare Earths Ltd., India, mass fraction 0.999) were homogenously mixed using an agate mortar and pestle. The mixtures were pelletized using a tungsten carbide lined steel die at a pressure of 20 MPa. The pellets were first heated at 1100 K for 24 h. Then, the resultant products were ground, again pelletized and further heated at 1200 K for 48 h. The individual compounds were characterized by X-ray powder diffraction technique using STOE powder diffractometer with Cu Kα radiation and graphite monochromator and found to be pure crystalline phases of $BaCeO_3(s)$, $SrCeO_3(s)$ and $Sr_2CeO_4(s)$.

Chemical analysis of all the synthesized samples was carried out using EDXRF method. The alkaline earth to cerium metal ratio obtained from EDXRF analysis was found to be the same as the formula ratio indicating that the compounds are stoichiometric with respect to metals.

Phase mixtures of $\{BaCeO_3(s) + BaCO_3(s) + CeO_2(s)\}$, $\{SrCeO_3(s) + SrCO_3(s) + CeO_2(s)\}$, $\{Sr_2CeO_4(s) + 2SrCO_3(s) + CeO_2(s)\}$ and $\{Sr_2CeO_4(s) + SrCO_3(s) + SrCeO_3(s)\}$ were prepared by homogenously mixing the individual oxides for KEQMS experiment. The pellets of different phase mixtures were then broken into small pieces and kept in a desiccator for measurement of partial pressures of $CO_2(g)$.

2.2. Knudsen effusion quadrupole mass spectrometry (KEQMS)

In this study, a Residual Gas Analyzer (RGA) based on quadrupole mass spectrometer coupled to a Knudsen effusion system was used for equilibrium partial pressure measurements. The details of the experimental setup and the calibration procedure of the experimental setup have been described by Rakshit et al. [16]. The temperature near the Knudsen cell was measured using a pre-calibrated (ITS-90) chromel–alumel thermocouple. The Knudsen cell used was made of 15 mol% calcia stabilized zirconia (CSZ) with a thin cylindrical orifice of diameter 0.8 mm and height 0.2 mm at the centre of the lid. The detected signal (I_i^+) measured using a Faraday cup detector is related to the partial pressure of the vapor species (p_i) by:

$$p_i = \frac{K_{inst} \cdot I_i^+ \cdot T}{\sigma_i \cdot a_i} \quad (1)$$

where K_{inst} is the instrumental constant, I_i^+ is the measured ion current in ampere, T is the absolute temperature near the Knudsen cell, σ_i is the electron impact cross-section and a_i isotopic abundance of the specific ion. Eq. (1) can be represented as;

$$\ln p_i = \ln K_{inst} + \ln(I_i^+ \cdot T) - \ln \sigma_i - \ln a_i \quad (2)$$

Eq. (2) is used to calculate the instrument constant (K_{inst}) by calibrating with a standard having known partial pressures at different temperatures. Prior to calibration of the instrument, the background signals were monitored by heating the Knudsen cell chamber with empty Knudsen cell at different temperatures from ambient to 1161 K at pressure level $\sim 1 \times 10^{-5}$ Pa. The background signals as a function of temperature are shown in Fig. 1. It is evident from the figure that the background signals corresponding to H_2^+, N_2^+, CO^+ and CO_2^+ do not change appreciably with change in temperature. During experiments, the actual signals were obtained by subtracting the ion intensities due to background.

The instrument was first calibrated using the phase mixture $\{BaCO_3(s) + BaO(s)\}$ at 30 eV ionization energy and keeping the other ion optic parameters constant for all sets of measurements. The experimental setup and the calibration constant thus calculated was checked by measuring the partial pressure of $CO_2(g)$ '$\{p(CO_2)\}$' over the phase mixture of $\{SrCO_3(s) + SrO(s)\}$. After validation of the method, $p(CO_2)$ were measured over the equilibrium phase mixtures of $\{BaCeO_3(s) + BaCO_3(s) + CeO_2(s)\}$ and $\{SrCeO_3(s) + SrCO_3(s) + CeO_2(s)\}$. There are two ways to prepare $Sr_2CeO_4(s)$: (i) by mixing stoichiometric ratios of $SrCO_3(s)$ and $CeO_2(s)$ and (ii) by successive addition of $SrCO_3(s)$ in $SrCeO_3(s)$. Hence, the values of $p(CO_2)$ were measured over both the equilibrium phase mixtures of $\{Sr_2CeO_4(s) + 2SrCO_3(s) + CeO_2(s)\}$ and $\{Sr_2CeO_4(s) + SrCO_3(s) + SrCeO_3(s)\}$.

3. Results and discussion

3.1. Calibration of KEQMS setup

The individual ion intensities of CO_2^+ peak over the equilibrium phase mixture of $\{BaCO_3(s) + BaO(s)\}$ were recorded at different temperatures for two successive runs and tabulated in Table 1. The individual ion intensities were least squares fitted as a function of temperature and is represented as:

$$\ln(IT) = \frac{-31541\ (\pm 414)}{T} + 15.94\ (\pm 0.44) \quad (852\text{–}1029\ \mathrm{K}) \quad (3)$$

Values of $\ln(K_{inst})$ as a function of temperature were calculated using Eqs. (2) and (3), the $CO_2(g)$ pressure for the equilibrium mixture $\{BaCO_3(s) + BaO(s)\}$ from literature [17] and $\ln\{\sigma(i = CO_2)\} = -45.52$ at 30 eV. The expression for $\ln(K_{inst})$ as a function of temperature is represented as:

$$\ln(K_{inst}) = \frac{-12}{T(\mathrm{K})} - 42.02 \quad (4)$$

The ion intensities of CO_2^+ over $\{SrCO_3(s) + SrO(s)\}$ were measured as a function of temperature and are given in Table 1. The individual ion intensities were least squares fitted as a function of temperature and are represented as:

$$\ln(IT) = \frac{-29426(\pm 641)}{T} + 15.50(\pm 0.71) \quad (849 - 965\ \mathrm{K}) \quad (5)$$

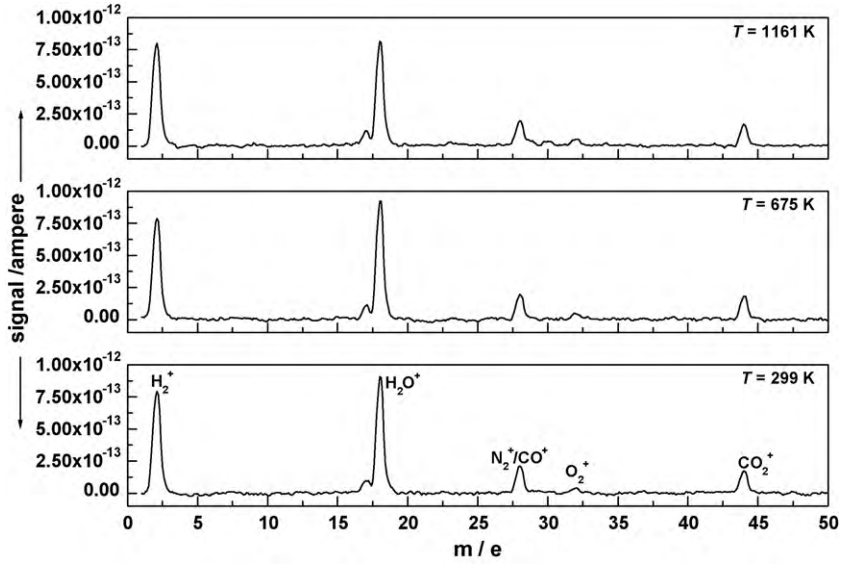

Fig. 1. Background mass spectra at different temperature using KEQMS with empty Knudsen cell.

Table 1
Ion intensities of CO_2^+ peak over equilibrium phase mixtures as a function of temperature.

{$BaCO_3$(s) + BaO(s)}				{$SrCO_3$(s) + SrO(s)}			
T (K)	I (A)	T (K)	I (A)	T (K)	I (A)	T (K)	I (A)
1*st run*		2*nd run*		1*st run*		2*nd run*	
852	1.04E−12	864	1.59E−12	849	8.08E−12	856	7.42E−12
876	1.99E−12	891	3.93E−12	864	1.04E−11	869	1.07E−11
896	3.85E−12	905	6.78E−12	878	1.60E−11	884	1.82E−11
942	2.33E−11	949	3.41E−11	922	8.47E−11	927	8.95E−11
952	3.31E−11	963	5.86E−11	935	1.41E−10	941	1.62E−10
968	6.03E−11	975	8.76E−11	950	2.13E−10	957	2.35E−10
981	9.03E−11	990	1.52E−10	960	2.96E−10	965	3.34E−10
993	1.37E−10	1003	2.12E−10				
1000	1.70E−10	1018	2.86E−10				
1020	2.70E−10	1027	3.57E−10				
1029	4.00E−10						

The values of ln{p(CO_2 (atm))} for the phase mixture {$SrCO_3$(s) + SrO(s)} was calculated by using Eqs. (2), (4) and (5). The corresponding expression is given as:

$$\ln\{p(CO_2(atm))\} = \frac{-29438\ (\pm 763)}{T} + 19.00(\pm 0.84) \quad (849 - 965\ K) \tag{6}$$

The CO_2(g) pressure was generated over this phase mixture due the equilibrium reaction:

$$SrCO_3(s) = SrO(s) + CO_2(g) \tag{7}$$

The enthalpy change associated with reaction (7) at the average experimental temperature was calculated using Eq. (6) and found to be $\Delta_r H_m^\circ$ (907 K) = (245 ± 6) kJ mol^{-1}, which is in good agreement with that of literature (239 kJ mol^{-1}) [17].

3.2. Measurement of partial pressure of CO_2(g) over equilibrium phase mixtures of strontium and barium cerates

Huang et al. [18] have reported the thermodynamic data of $Na_4Fe_6O_{11}$(s) by measuring the partial pressure of CO_2(g) over {$2Na_2CO_3$(s) + $3Fe_2O_3$(s)} phase mixture using Knudsen effusion mass spectrometry. Similar approach was adopted in this study to determine the Gibbs energies of formation of $BaCeO_3$(s), $SrCeO_3$(s) and Sr_2CeO_4(s) by measuring the partial pressure of CO_2(g) over the equilibrium phase mixtures of {$BaCeO_3$(s) + $BaCO_3$(s) + CeO_2(s)}, {$SrCeO_3$(s) + $SrCO_3$(s) + CeO_2(s)}, {Sr_2CeO_4(s) + 2$SrCO_3$(s) + CeO_2(s)} and {Sr_2CeO_4(s) + $SrCO_3$(s) + $SrCeO_3$(s)}. After the mass spectrometric measurements, the resultant phase mixtures were analyzed by X-ray powder diffraction technique and found to contain the same phases and therefore, it was assumed that the following equilibrium reactions were established inside the Knudsen cell under experimental conditions.

$$ACO_3(s) + CeO_2(s) = ACeO_3(s) + CO_2(g) \quad (A = Sr, Ba) \tag{8}$$

$$ACO_3(s) + ACeO_3(s) = A_2CeO_4(s) + CO_2(g) \quad (A = Sr) \tag{9}$$

Therefore, the measured p(CO_2) corresponds to the equilibrium pressures of the above reactions.

3.2.1. $p(CO_2)$ over the phase mixtures {$BaCeO_3$(s) + $BaCO_3$(s) + CeO_2(s)} and {$SrCeO_3$(s) + $SrCO_3$(s) + CeO_2(s)}

The ion intensities of CO_2^+ peak due to the equilibrium reaction (8) (A = Ba, Sr) were measured as a function of temperature and are given in Table 2. The p(CO_2) values were calculated by using the ion intensities and Eqs. (2) and (4). The variation of ln{p(CO_2 (atm))} as a function of temperature for both the ternary phase mixtures are shown in Figs. 2 and 3, respectively. The ln{p(CO_2 (atm))} values for both the phase mixtures for two successive runs were least squares fitted as a function of temperature and are represented below.

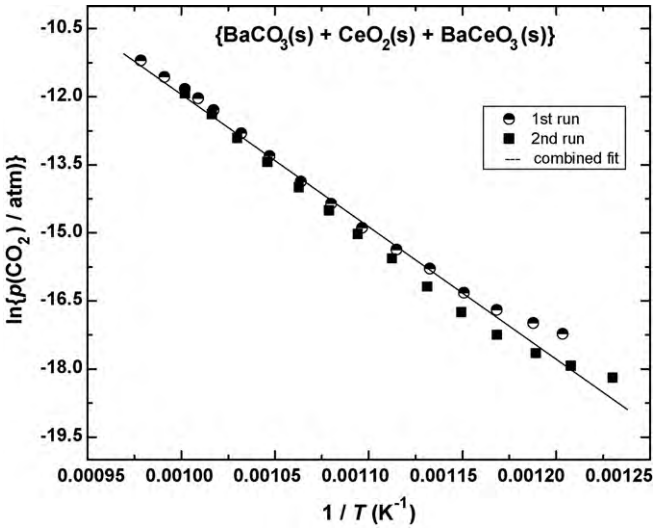

Fig. 2. Plot of ln{p(CO_2)} versus temperature for {$BaCeO_3$(s) + $BaCO_3$(s) + CeO_2(s)}.

For the phase mixture {$BaCeO_3$(s) + $BaCO_3$(s) + CeO_2(s)}:

$$\ln\{p(CO_2(atm))\} = \frac{-28891\ (\pm 665)}{T} + 16.91(\pm 0.73)$$
$$(813 \le T\ (K) \le 1022) \tag{10}$$

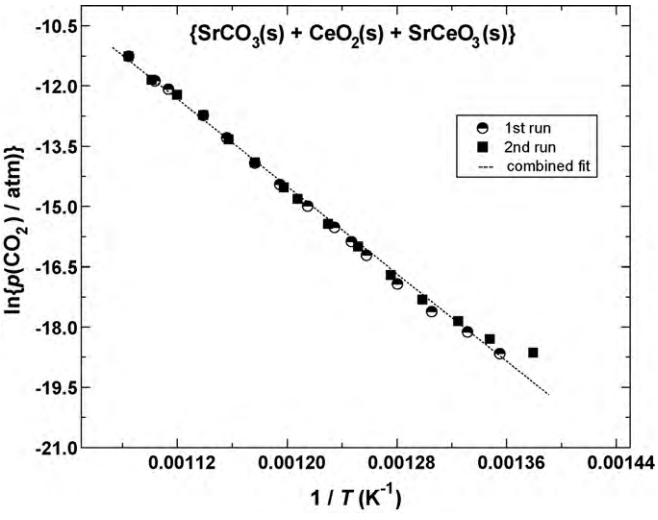

Fig. 3. Plot of ln{p(CO_2)} versus temperature for {$SrCeO_3$(s) + $SrCO_3$(s) + CeO_2(s)}.

Table 2
$p(CO_2)$ values as a function of temperature for equilibrium phase mixtures for barium and strontium cerate.

{$BaCeO_3(s)+BaCO_3(s)+CeO_2(s)$}			{$SrCeO_3(s)+SrCO_3(s)+CeO_2(s)$}		
T (K)	I (A)	$p(CO_2)$ (atm)	T (K)	I (A)	$p(CO_2)$ (atm)
1*st run*			1*st run*		
831	1.22E−12	3.311E−8	738	3.26E−13	7.843E−9
842	1.53E−12	4.208E−8	751	5.52E−13	1.352E−8
856	2.01E−12	5.621E−8	766	8.94E−13	2.234E−8
869	2.89E−12	8.206E−8	781	1.75E−12	4.459E−8
883	4.83E−12	1.394E−7	795	3.47E−12	9.003E−8
897	7.22E−12	2.117E−7	802	4.85E−12	1.270E−7
912	1.15E−11	3.429E−7	810	6.83E−12	1.806E−7
926	1.92E−11	5.814E−7	823	1.14E−11	3.063E−7
940	3.08E−11	9.470E−7	837	1.93E−11	5.276E−7
955	5.33E−11	1.665E−6	850	3.25E−11	9.024E−7
969	8.69E−11	2.755E−6	865	5.97E−11	1.687E−6
983	1.43E−10	4.600E−6	878	1.03E−10	2.955E−6
991	1.84E−10	5.968E−6	898	1.93E−10	5.666E−6
998	2.24E−10	7.317E−6	906	2.36E−10	6.991E−6
1009	2.88E−10	9.513E−6	922	4.28E−10	1.290E−5
1022	4.09E−10	1.369E−5	2*nd run*		
2*nd run*			725	3.42E−13	8.081E−9
813	4.75E−13	1.261E−8	742	4.69E−13	1.135E−8
828	6.07E−13	1.641E−8	755	7.20E−13	1.773E−8
841	7.84E−13	2.154E−8	770	1.20E−12	3.014E−8
856	1.16E−12	3.244E−8	784	2.18E−12	5.577E−8
870	1.87E−12	5.316E−8	799	4.29E−12	1.119E−7
884	3.24E−12	9.361E−8	813	7.42E−12	1.969E−7
899	5.96E−12	1.752E−7	828	1.36E−11	3.677E−7
914	1.00E−11	2.989E−7	835	1.80E−11	4.909E−7
927	1.65E−11	5.002E−7	850	3.30E−11	9.163E−7
941	2.72E−11	8.372E−7	864	5.78E−11	1.632E−6
956	4.69E−11	1.467E−6	878	1.04E−10	2.984E−6
971	7.81E−11	2.481E−6	893	1.69E−10	4.933E−6
984	1.30E−10	4.186E−6	908	2.42E−10	7.184E−6
998	2.03E−10	6.631E−6	922	4.29E−10	1.293E−5

For the phase mixture {$SrCeO_3(s)+SrCO_3(s)+CeO_2(s)$}:

$$\ln\{p(CO_2(\text{atm}))\} = \frac{-27056\,(\pm390)}{T} + 17.96(\pm0.48)$$
$$(725 \le T\,(\text{K}) \le 922) \qquad (11)$$

The thermodynamic stability of $ACeO_3$ with respect to the formation of the corresponding carbonates ACO_3 is depicted in Fig. 4. The lines show the boundary of stable region of $ACeO_3$ (A = Ba, Sr). The thermodynamically stable region for cerates lies below the line, whereas above the line $ACeO_3$ will form ACO_3 and CeO_2 in presence of CO_2(g). The figure also indicates the chemical stability order of cerates against CO_2 and predicts that $SrCeO_3$ is more stable compared to $BaCeO_3$.

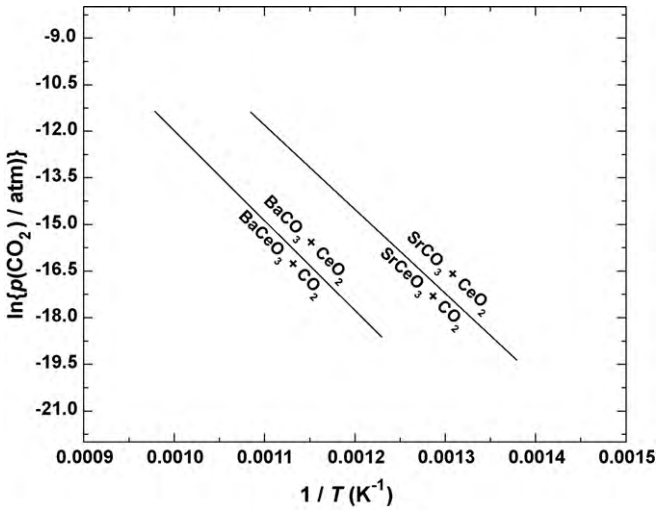

Fig. 4. Stability region plot of $ACeO_3$ (A = Ba, Sr) with respect to ACO_3.

The enthalpy changes due to reaction (8) for (A = Ba, Sr) at the average temperature of measurement were found to be $\Delta_r H_m^\circ$ (918 K) = (240 ± 6) kJ mol^{-1} for A = Ba and $\Delta_r H_m^\circ$ (824 K) = (225 ± 3) kJ mol^{-1} for A = Sr. The standard Gibbs energy of reaction (8) for (A = Ba) is calculated as:

$$\Delta_r G_m^\circ(T)(\text{kJ mol}^{-1})(\pm6) = 240–0.1406\cdot(T\,(\text{K}))$$
$$(813 \le T\,(\text{K}) \le 1022) \qquad (12)$$

The standard Gibbs energy of reaction (8) for (A = Sr) is calculated as:

$$\Delta_r G_m^\circ(T)(\text{kJ mol}^{-1})(\pm3) = 225–0.1493\cdot(T\,(\text{K}))$$
$$(725 \le T\,(\text{K}) \le 922) \qquad (13)$$

The standard molar Gibbs energies of formation ($\Delta_f G_m^\circ$) of $BaCeO_3$(s) and $SrCeO_3$(s) from the elements were calculated from Eqs. (12) and (13) and the values of $\Delta_f G^o{}_m(T)$ for CO_2(g), $BaCO_3$(s), $SrCO_3$(s) and CeO_2(s) given in Table 3. The corresponding expres-

Table 3
Standard molar Gibbs energy of formation, $\Delta_f G_m^\circ(T)$, of different compounds used for calculation in this study taken from literature [17].

Compound	$\Delta_f G_m^\circ(T)$ (kJ mol^{-1}) (700–1000 K)
CO_2(g)	−394 − 0.0019·(T(K))
$BaCO_3$(s)	−1206 + 0.2546·(T(K))
$SrCO_3$(s)	−1223 + 0.2627·(T(K))
CeO_2(s)	−1086 + 0.2074·(T(K))

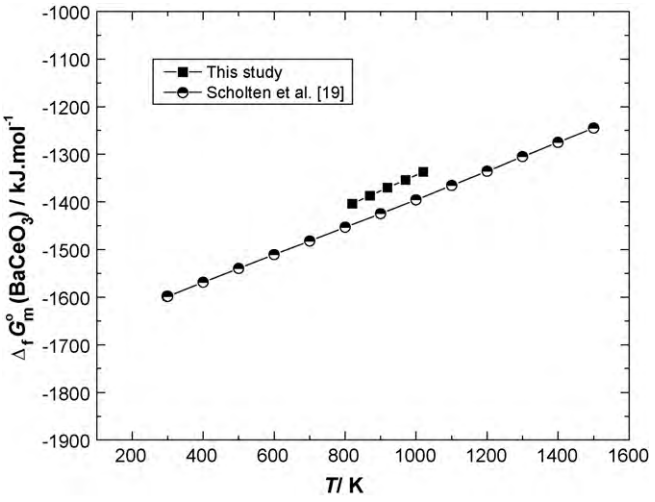

Fig. 5. Comparison of $\Delta_f G_m^\circ(T)$ for $BaCeO_3$(s).

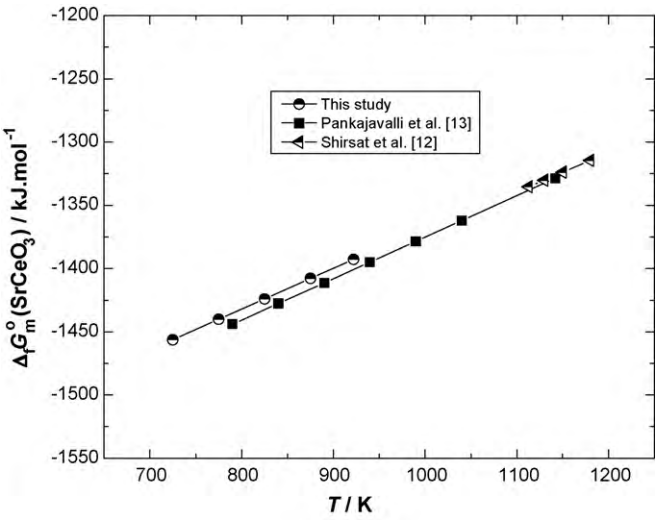

Fig. 6. Comparison of $\Delta_f G_m^\circ(T)$ for $SrCeO_3$(s).

sions are:

$$\Delta_f G_m^\circ(BaCeO_3,\ s, T)(kJ\,mol^{-1})(\pm 6) = -1675.3 + 0.3315\cdot(T(K)) \quad (813 \le T(K) \le 1022) \tag{14}$$

$$\Delta_f G_m^\circ(SrCeO_3,\ s, T)(kJ\,mol^{-1})(\pm 3) = -1690.3 + 0.3227\cdot(T(K)) \quad (725 \le T(K) \le 922) \tag{15}$$

Scholten et al. [19] have estimated the $\Delta_f G_m^\circ(T)$ for $BaCeO_3$(s) using their enthalpy increment data and other auxiliary data from the literature from 298.15 to 1500 K. The $\Delta_f G_m^\circ(T)$ for $BaCeO_3$(s) from Eq. (14) are compared with that of above literature and represented in Fig. 5. The values of $\Delta_f G_m^\circ(T)$ for $BaCeO_3$(s) in this study is ~50 kJ mol^{-1} more negative compared to the estimated literature values [19].

Shirsat et al. [12] have measured the partial pressure of CO_2(g) over the phase mixture {$SrCeO_3$(s) + $SrCO_3$(s) + CeO_2(s)} by tensimetric measurements in the temperature range 1113 K to 1184 K and calculated $\Delta_f G_m^\circ(T)$ for $SrCeO_3$(s). Pankajavalli et al. [13] have determined the $\Delta_f G_m^\circ(T)$ for $SrCeO_3$(s) using solid-state electrochemical cell experiments from 788 to 1142 K. The values of $\Delta_f G_m^\circ(T)$ for $SrCeO_3$(s) obtained in this study are compared with the values reported in literature [12,13] and shown in Fig. 6. The figure shows that the $\Delta_f G_m^\circ(T)$ for $SrCeO_3$(s) are in good agreement with that of literature.

The Standard molar Gibbs energy of formation ($\Delta_f G_m^\circ$) of $BaCeO_3$(s) and $SrCeO_3$(s) obtained in this study and the data reported in the literature are used to calculate the Gibbs energy change for reaction: $ACeO_3$(s) + CO_2(g) = ACO_3(s) + CeO_2(s) and are compared in Table 4. It is observed that for A = Ba, the values of $\Delta_r G_m^\circ$ obtained in this study is ~60 kJ mol^{-1} more negative than that of Scholten et al. [19], whereas the values are in close agreement for A = Sr.

Table 4
Comparison of Gibbs energy change for reaction: $ACeO_3$(s) + CO_2(g) = ACO_3(s) + CeO_2(s).

Reaction	$\Delta_r G_m^\circ(T)$ (kJ mol^{-1})	Reference
A = Ba	−240.0 + 0.1406·(T(K))	This study
	−210.8 + 0.1713·(T(K))	Scholten et al. [19]
A = Sr	−225.0 + 0.1493·(T(K))	This study
	−211.6 + 0.1445·(T(K))	Pankajavalli et al. [13]
	−235.0 + 0.1620·(T(K))	Shirsat et al. [12]

3.2.2. $p(CO_2)$ over the phase mixtures {Sr_2CeO_4(s) + 2$SrCO_3$(s) + CeO_2(s)} and {Sr_2CeO_4(s) + $SrCO_3$(s) + $SrCeO_3$(s)}

Two different phase mixtures {Sr_2CeO_4(s) + 2$SrCO_3$(s) + CeO_2(s)} and {Sr_2CeO_4(s) + $SrCO_3$(s) + $SrCeO_3$(s)} were chosen for KEQMS experiments. After the KEQMS experiments, the resultant samples were characterized by X-ray diffraction technique and found to be the same mixture as taken before the experiments. Hence, the equilibrium reactions for both the phase mixture can be written as:

$$2SrCO_3(s) + CeO_2(s) = Sr_2CeO_4(s) + 2CO_2(g) \tag{16}$$

$$SrCO_3(s) + SrCeO_3(s) = Sr_2CeO_4(s) + CO_2(g) \tag{17}$$

The ion intensities of CO_2^+ peak due to the above equilibrium reactions were measured as a function of temperature and are given in Table 5. The $p(CO_2)$ values were calculated using the ion intensities data from Table 4 and Eqs. (2) and (4). The variation of ln{$p(CO_2$ (atm))} as a function of temperature for both the ternary phase mixtures are shown in Figs. 7 and 8, respectively. The ln{$p(CO_2$ (atm))} values for both the phase mixtures for two successive runs were least squares fitted as a function of temperature and are represented as:

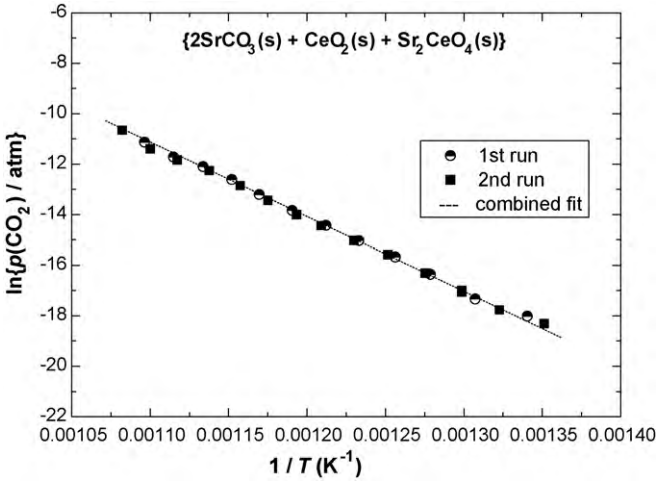

Fig. 7. ln{$p(CO_2)$} as a function of temperature for {Sr_2CeO_4(s) + 2$SrCO_3$(s) + CeO_2(s)}.

Table 5
$p(CO_2)$ values as a function of temperature for equilibrium phase mixtures for $Sr_2CeO_4(s)$.

{$Sr_2CeO_4(s)+2SrCO_3(s)+CeO_2(s)$}			{$Sr_2CeO_4(s)+SrCO_3(s)+SrCeO_3(s)$}		
T (K)	I (A)	$p(CO_2)$ (atm)	T (K)	I (A)	$p(CO_2)$ (atm)
1*st run*			1*st run*		
746	6.17E−13	1.500E−8	776	1.80E−12	4.555E−8
765	1.19E−12	2.968E−8	795	2.87E−12	7.443E−8
782	3.08E−12	7.855E−8	813	5.59E−12	1.483E−7
796	6.02E−12	1.563E−7	833	1.19E−11	3.236E−7
811	1.12E−11	2.964E−7	853	2.63E−11	7.325E−7
825	2.01E−11	5.412E−7	873	5.79E−11	1.651E−6
840	3.55E−11	9.735E−7	891	1.17E−10	3.406E−6
855	6.59E−11	1.840E−6	910	2.41E−10	7.167E−6
868	1.18E−10	3.345E−6	931	4.35E−10	1.324E−5
882	1.93E−10	5.561E−6	943	7.30E−10	2.251E−5
897	2.79E−10	8.177E−6	2*nd run*		
912	4.93E−10	1.469E−5	781	1.26E−12	3.209E−8
2*nd run*			793	1.86E−12	4.811E−8
740	4.61E−13	1.112E−8	809	3.59E−12	9.476E−8
756	7.80E−13	1.922E−8	822	6.59E−12	1.768E−7
770	1.55E−12	3.891E−8	838	1.25E−11	3.420E−7
770	1.66E−12	4.167E−8	852	2.17E−11	6.037E−7
784	3.23E−12	8.259E−8	865	3.54E−11	1.000E−6
799	6.57E−12	1.712E−7	880	6.64E−11	1.909E−6
813	1.13E−11	2.998E−7	895	1.16E−10	3.392E−6
827	1.99E−11	5.371E−7	910	1.96E−10	5.829E−6
838	3.02E−11	8.262E−7	925	2.80E−10	8.466E−6
851	5.24E−11	1.456E−6	938	4.13E−10	1.267E−5
864	9.27E−11	2.616E−6	952	7.67E−10	2.388E−5
879	1.66E−10	4.766E−6			
895	2.46E−10	7.194E−6			
909	3.80E−10	1.129E−5			
924	7.82E−10	2.362E−5			

For the phase mixture {$Sr_2CeO_4(s)+2SrCO_3(s)+CeO_2(s)$}:

$$\ln\{p(CO_2(atm))\} = \frac{-28746(\pm211)}{T} + 20.38(\pm0.26)$$
$$(740 \le T(K) \le 924) \quad (18)$$

and for the phase mixture {$Sr_2CeO_4(s)+SrCO_3(s)+SrCeO_3(s)$}:

$$\ln\{p(CO_2(atm))\} = \frac{-28405(\pm512)}{T} + 19.17(\pm0.6)$$
$$(776 \le T(K) \le 952) \quad (19)$$

The enthalpy changes due to reactions (16) and (17) at the average temperature of measurement were determined and found to be $\Delta_{r(16)}H_m^\circ$ (832 K) = (478 ± 4) kJ mol^{-1} and $\Delta_{r(17)}H_m^\circ$ (864 K) = (236 ± 4) kJ mol^{-1}. The standard Gibbs energies of reactions (16) and (17) are calculated and represented as:

$$\Delta_{r(16)}G_m^\circ(T)(kJ\,mol^{-1})(\pm2) = 478 - 0.3389\cdot(T(K))$$
$$(740 \le T(K) \le 924) \quad (20)$$

and

$$\Delta_{r(17)}G_m^\circ(T)(kJ\,mol^{-1})(\pm4) = 236 - 0.1594\cdot(T(K))$$
$$(776 \le T(K) \le 952) \quad (21)$$

The $\Delta_fG_m^\circ$ of $Sr_2CeO_4(s)$ from the elements calculated using $\Delta_{r(16)}G_m^\circ(T)$ and the values of $\Delta_fG_m^\circ(T)$ for $CO_2(g)$, $SrCO_3(s)$ and $CeO_2(s)$ from Table 3 is given as:

$$\Delta_fG_m^\circ(Sr_2CeO_4,\ s, T)(kJ\,mol^{-1})(\pm3) = -2266 + 0.3977\cdot(T(K))$$
$$(740 \le T(K) \le 924) \quad (22)$$

Similarly, the $\Delta_fG_m^\circ$ of $Sr_2CeO_4(s)$ from the elements calculated using $\Delta_{r(17)}G_m^\circ(T)$ and the values of $\Delta_fG_m^\circ(T)$ for $CO_2(g)$, $SrCO_3(s)$ from Table 3 and for $SrCeO_3(s)$ from Eq. (15) is given as:

$$\Delta_fG_m^\circ(Sr_2CeO_4,\ s, T)(kJ\,mol^{-1})(\pm4) = -2283.0 + 0.4279\cdot(T(K))$$
$$(776 \le T(K) \le 952) \quad (23)$$

Pankajavalli et al. [13] have determined the $\Delta_fG_m^\circ(T)$ of $Sr_2CeO_4(s)$ using solid-state galvanic cell technique from 805 to 1066 K. Shirsat et al. [14] have determined the $\Delta_fG_m^\circ(T)$ of $Sr_2CeO_4(s)$ using tensimetric technique from 1035 to 1115 K. The individual values of $\Delta_fG_m^\circ(T)$ for $Sr_2CeO_4(s)$ were compared along with this study (Eqs. (22) and (23)) and shown in Fig. 9. It can be seen from Fig. 9 that values of $\Delta_fG_m^\circ(T)$ of $Sr_2CeO_4(s)$ determined from both the phase mixture using KEQMS technique are in very good agreement with that of literature [13,14]. Hence, $\Delta_fG_m^\circ(T)$ of $Sr_2CeO_4(s)$ from Eqs. (22), (23) and that of literature [13,14] were least squares fitted as a function of temperature and are represented as:

$$\Delta_fG_m^\circ(Sr_2CeO_4,\ s, T)(kJ\,mol^{-1})(\pm9) = -2273.0 + 0.4077\cdot(T(K))$$
$$(740 \le T(K) \le 1115) \quad (24)$$

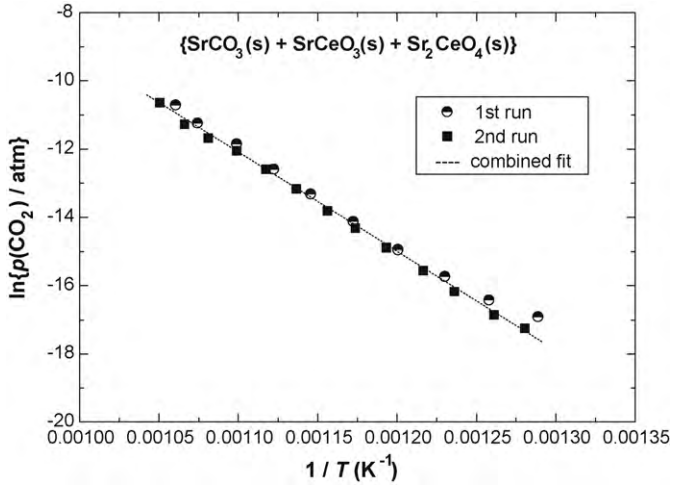

Fig. 8. $\ln\{p(CO_2)\}$ as a function of temperature for {$Sr_2CeO_4(s)+SrCO_3(s)+SrCeO_3(s)$}.

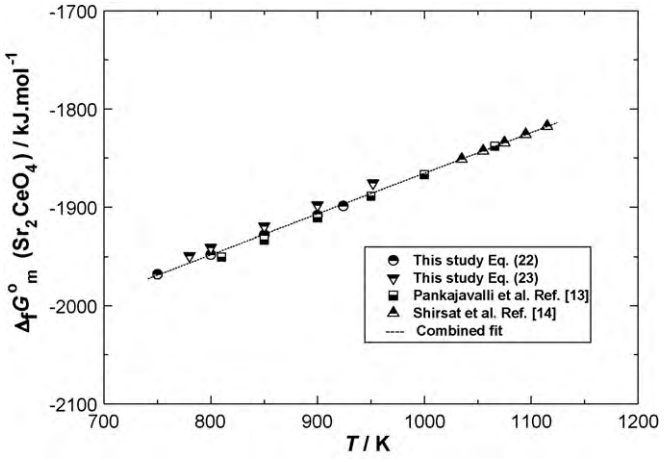

Fig. 9. Comparison of $\Delta_fG_m^\circ(T)$ for $Sr_2CeO_4(s)$.

3.3. Comparison of $\Delta_fH_m^\circ$ (298.15 K) for $BaCeO_3(s)$, $SrCeO_3(s)$ and $Sr_2CeO_4(s)$

Scholten et al. [19] have reported smoothed values of thermodynamic functions for $BaCeO_3(s)$ based on their low temperature heat capacity data and high temperature enthalpy increment data

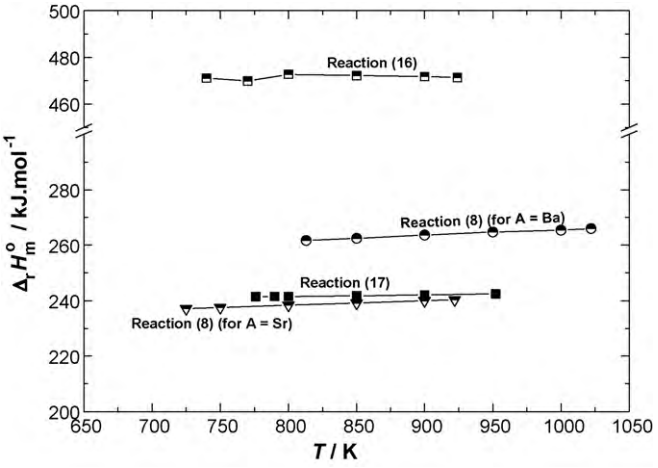

Fig. 10. Third law values of $\Delta_r H_m^\circ(T)$ for reactions (8) (for A = Ba, Sr), (16) and (17).

Table 6
$\Delta_f H_m^\circ$ (298.15 K) of $BaCeO_3$(s), $SrCeO_3$(s) and Sr_2CeO_4(s).

Compound	$\Delta_f H_m^\circ$ (298.15 K) (kJ mol^{-1})	Reference
$BaCeO_3$(s)	−1644 (±6)	This study
	−1686.5 (±3.9)	Scholten et al. [19]
	−1690.0 (±2.5)	Cordfunke et al. [20]
$SrCeO_3$(s)	−1685.2 (±3)	This study
	−1675.3 (±10.8), −1676.3 (±12.8)	Pankajavalli et al. [13]
	−1687.1 (±2.7)	Cordfunke et al. [20]
	−1685.6 (±3.8)	Goudiakas et al. [21]
Sr_2CeO_4(s)	−2286.1 (±3)	This study {Eq. (16)}
	−2276.8 (±4)	This study {Eq. (17)}
	−2293.7 (±21)	Pankajvalli et al. [13]
	−2272.5 (±7)	Shirsat et al. [14]
	−2277.3 (±3)	Ali et al. [22]
	−2280.8 (Estimated)	Yokokawa et al. [23]

from drop calorimetry. Pankajavalli et al. [13] have determined the $\Delta_f H_m^\circ$ (298.15 K) for $SrCeO_3$(s) and Sr_2CeO_4(s) based on their emf data and compared with that of literature [20,21]. Shirsat et al. [14] have determined the $\Delta_f H_m^\circ$ (298.15 K) for Sr_2CeO_4(s) based on their tensimetry data and compared with that of literature [13,22,23]. In this study, $\Delta_f H_m^\circ$ (298.15 K) for $BaCeO_3$(s), $SrCeO_3$(s) and Sr_2CeO_4(s) were determined using 3rd law analysis by using partial pressure of CO_2(g) over the equilibrium reactions (8) (for A = Ba, Sr), for reactions (16) and (17). The auxiliary data for 3rd law calculations were taken from literature [17]. The values of $\Delta_r H_m^\circ$ (298.15 K) for the reactions (8) (for A = Ba, Sr), (16) and (17) were plotted as a function of experimental temperature and shown in Fig. 10. No systematic trend in the values of $\Delta_r H_m^\circ$ (298.15 K) was observed for all these above reactions. Hence, the average value of $\Delta_r H_m^\circ$ (298.15 K) was used to calculate the $\Delta_f H_m^\circ$ (298.15 K) for the respective compound. The average value of $\Delta_f H_m^\circ$ (298.15 K) for all the compounds is listed in Table 6 along with that of literature. These values show that the $\Delta_f H_m^\circ$ (298.15 K) for $BaCeO_3$(s) is more positive by 42 kJ mol^{-1} and those for $SrCeO_3$(s) and Sr_2CeO_4(s) are in very good agreement with those reported in literature.

4. Conclusions

The partial pressures of CO_2(g) over the equilibrium phase mixtures of {$BaCeO_3$(s) + $BaCO_3$(s) + CeO_2(s)} and {$SrCeO_3$(s) + $SrCO_3$(s) + CeO_2(s)} were calculated at the usual fuel cell operating temperature of 900 K and found to be 2.5×10^{-7} and 5.5×10^{-6} atm, respectively. These values suggest that $BaCeO_3$ is more prone to form carbonate compared to $SrCeO_3$. The Gibbs free energies of formation of $BaCeO_3$ and $SrCeO_3$ from their elements also indicate that $SrCeO_3$ is more stable compared to $BaCeO_3$. Third law analysis also shows that partial pressure of CO_2(g) over the different phase mixtures were reliable.

References

[1] J. Fronlentier, M. Henault, Solid State Ionics 9–10 (1993) 1277.
[2] T. Inone, N. Seki, K. Eguchi, H. Arai, J. Electrochem. Soc. 137 (1990) 2523.
[3] S. Hamakawa, T. Hayakawa, A.P.E. York, T. Tsamoda, Y.S. Yoon, K. Suzuki, M. Shimizu, K. Takohira, J. Electrochem. Soc. 143 (1996) 1264.
[4] T. Mori, J. Drennan, Y. Wang, J.G. Li, T. Ikegami, J. Therm. Anal. Calorim. 70 (2002) 309.
[5] P. Sulcova, M. Trojan, J. Therm. Anal. Calorim. 65 (2001) 399.
[6] F. Lefebvre-Joud, G. Gauthier, J. Mougin, J. Appl. Electrochem. 39 (2009) 535.
[7] A.B. Stambouli, E. Traversa, Ren. Sustain. Ener. Rev. 6 (2002) 433.
[8] T. Norby, Solid State Ionics 125 (1999) 1.
[9] H. Iwahara, Solid State Ionics 9 (1996) 86.
[10] E. Danielson, M. Devenny, D.M. Giaquinta, J.H. Golden, R.C. Hanshalter, E.W. McFarland, D.M. Poojary, C.M. Reaves, W.H. Weimberg, X.D. Wu, Science 279 (1998) 837.
[11] R. Sankar, G.V. Subba Rao, J. Electrochem. Soc. 147 (2000) 2773.
[12] A.N. Shirsat, K.N.G. Kaimal, S.R. Bharadwaj, D. Das, J. Solid State Chem. 177 (2004) 2007.
[13] R. Pankajavalli, K. ananthasivan, S. anthonysamy, P.R. Vasudeva Rao, J. Nucl. Mater. 336 (2005) 177.
[14] A.N. Shirsat, K.N.G. Kaimal, S.R. Bharadwaj, D. Das, Thermochim. Acta 447 (2006) 101.
[15] L. Jingde, W. Ling, F. Lihua, L. Yuehua, D. Lei, G. Hongxia, J. Rare Earths 26 (2008) 505.
[16] S.K. Rakshit, Y.P. Naik, S.C. Parida, Smruti Dash, Ziley Singh, B.K. Sen, V. Venugopal, J. Solid State Chem. 181 (2008) 1402.
[17] M.W. Chase Jr., JANAF Thermochemical Tables, 4th ed., J. Phys. Chem. Ref. Data 23 (1995) Monograph No. 9.
[18] J. Huang, T. Furkawa, K. Aoto, J. Chem. Thermodyn. 38 (2006) 1.
[19] M.J. Scholten, J. Schoonman, J.C. van Miltenburg, E.H.P. Cordfunke, Thermochim. Acta 268 (1995) 161.
[20] E.H.P. Cordfunke, A.S. Booii, M.E. Huntelaar, J. Chem. Thermodyn. 30 (1998) 437.
[21] J. Goudiakas, R.G. Haire, J. Fuger, J. Chem. Thermodyn. 22 (1990) 577.
[22] M. Ali (Basu), R.V. Wandekar, S.R. Bharadwaj, D. Das, J. Thermal. Anal. Calorim. 78 (2004) 715.
[23] H. Yokokawa, N. Sakai, T. Kawada, M. Dokiya, J. Solid State Chem. 94 (1991) 106.